2nd International Joint Conference on Water Distribution Systems Analysis & Computing and Control in the Water Industry
Valencia (Spain), 18-22 July 2022
doi: https://doi.org/10.4995/WDSA-CCWI2022.2022.14733

# PRESSURE SENSOR PLACEMENT IN WATER NETWORKS BASED ON SENSITIVITY MATRIX: A REAL INSTRUMENTATION PROJECT PLAN

**Joan Van Eeckhout[1], Josep Cugueró[2] and Ramon Pérez[3]**

[1,2,3] CS2AC, Universitat Politècnica de Catalunya. Rambla sant Nebridi 10, 08222, Terrassa, Spain
[1]Taigua, Aigua Municipal de Terrassa. Carrer de la Societat, 30, 08221 Terrassa, Spain

[1] *joan.van.eeckhout@upc.edul,*[2] *josep.cuguero@upc.edu,* [3] *ramon.perez@upc.edu.*

## Abstract

The instrumentation and supervision of water distribution networks (WDN) are challenging tasks as the use of monitoring devices imply a high cost including installation and maintenance. One of the emerging issues is the definition of the best possible layout of the measurements to be recorded. Considering the sampling costs and budget limitations on the number of sensors to be distributed, to determine a trade-off is mandatory. The trade-off may highly depend on the final use of these sensors. This work presents a methodology to support practitioners to decide which is the optimal pressure sensor placement and the appropriate number of pressure sensors to install on a WDN. Two main applications for demand calibration and leak detection and localisation are considered. A sensor placement methodology is applied to find the most sensible locations with respect to demand groups. Additionally, as the sensor placement methodology does not define an optimal number of sensors to be distributed in the WDN, an approach to formulate a trade-off is developed. This approach generates an indicator that quantifies the degree of relevance of the information recorded by a given sensor layout. The methodology presented is applied on a real WDN to select the most appropriate pressure measurement layout as part of an instrumentation project plan.

**Keywords**
Water Distribution Networks, Sampling design, Sensors.

## 1 INTRODUCTION

Water Distribution Networks (WDNs) generally are large and complex systems formed by thousands of pipes and nodes and its instrumentation and supervision are challenging tasks as the use of monitoring devices imply a high cost including installation and maintenance. One of the emerging issues is the definition of the best possible layout of the measurements to be recorded, as the number of measurement devices is far smaller than the potential measurement points [1]. The use of models is crucial in this process, even if the final application using these measurements might not be based on WDN models. However, the suitability of the layout of the sensors may depend on the final application using these sensors [2].

Within the framework of an industrial thesis, the municipal water company of Terrassa (TAIGUA) intends to calibrate its WDN models. An industrial thesis consists in a strategic research project of a company where a doctoral student develops his research training in collaboration with a university. Following the seven-step general calibration procedure proposed by Ormsbee and Lingireddy [3], considering the intended use of the models, three model use types were identified whose differences arise in the precision of the demand model [4]. Models of type one are used for planning purposes within a ten year horizon. Models of type two are intended to perform short term predictions in peak days and need a more precise demand model. Models of type three would allow leakage detection and localization and need telemeter measurements to be fed constantly.

To generate a type three model a microcalibration process has to be performed. This microcalibration process requires more instrumentation to be installed in the WDN. As one objective is to generate and calibrate different groups of demand in the same DMA [5] and pressure monitoring is much less expensive than flow monitoring [6], it is chosen to install pressure sensors within the DMAs. Furthermore, results presented in [7] show that for meshed networks measuring pressure seems to be the best option when calibrating geographical groups of demand.

The pressure sensors that will be installed are the remote transmission units with data loggers ADT1 [8]. Despite the usual versatility of the pressure loggers which allows to place them at hydrants or blow off valves and move them to other locations without the need of a construction project, the company has decided to install the pressure sensors directly at the distribution pipes by means of small valve boxes avoiding possible vandalism damage. However, by means of pressure drilling, also referred to as hot tapping, line tapping or pressure tapping, the pressure sensors will be directly installed at pressurized pipelines without having to drain down the system or interrupt the service. Therefore, the pressure sensors will be installed at fixed locations. This fact gives relevance to carry out a sampling design (SD).

When considering the sampling costs and budget limitations on the number of sensors to be distributed to determine a trade-off is mandatory. Generally, the trade-offs analysed in literature the balance the need for better-calibrated models with the SD costs to justify the expenses on sampling efforts and data collection [9], [10], [11], [12], [13], [14], [15]. However, Kang and Lansey [16] point out that considering the trade-off between model accuracy and precision is more appropriate for the optimal meter placement than considering and minimize the metering costs.

There is not a definitive guidance to practitioners on how to balance the SD costs and there is not much evidence that SD methodologies are being used in practice [17]. Therefore, it is necessary to develop a methodology that supports practitioners to decide which is the appropriate number of sensors to install on a WDN.

In this paper, with the aim to perform demand calibration with pressure sensors, a sensor placement methodology is applied to find the most sensible locations with respect to demand groups [5].

Additionally, as the sensor placement methodology does not define an optimal number of sensors to be distributed in the WDN, an approach to obtain a trade-off is developed. This approach generates an indicator that quantifies the degree of relevance of the information recorded by a given sensor layout.

As a leak-detection and localization approach can be coupled with the demand calibration methodology [18], the proposed indicator does not only consider or depend on a single final application. The procedure to generate this indicator is based on analysing the magnitude of the pressure changes that the sensors would measure when variations in the demand occur. Thus, comparing the values of the indicator for several layouts of sensors with different numbers of sensors distributed in the network, the optimal number of sensors can be defined.

The methodology presented in this paper is applied on a real WDN to select the most appropriate pressure measurement layout as part of an instrumentation project plan. The studied WDN supplies the northern urban area of Terrassa and consists of four District Metered Areas (DMAs) gravity-fed from a single tank. The two lower DMAs are separated by a pressure reducing valve (PRV) from the two upstream DMAs.

## 2 PROBLEM FORMALIZATION

Given a WDN and its EPANET model with all the physical behaviour well defined and validated in a macrocalibration phase (Water Distribution Network Model calibration and Continuous Maintenance: Terrassa, a real application), the expected nodal pressures can be obtained simulating this model. The simulation of a WDN model depend on the demands and the boundary conditions, as for instance the levels of the tanks or the status of the pumps and valves status. Equation (1) represents the process of obtaining the estimated nodal pressures vector $\hat{\mathbf{p}} \in \mathbb{R}^{N_n}$ through the simulation of the WDN model at the boundary conditions $B_{Cond}$ and nodal demands vector $\mathbf{d} \in \mathbb{R}^{N_n}$**.** Being $N_n$ the number of nodes of the WDN model.

$$Simulate\ Model(B_{Cond}, \mathbf{d}) = \hat{\mathbf{p}} \tag{1}$$

The relationship between pressures and demands is non-linear. However, given a working point $(B_{Cond}, \mathbf{d})$ a linear approximation can be obtained as shown in equation (2).

$$\Delta\hat{\mathbf{p}} = \mathbf{S}(B_{Cond}, \mathbf{d}) \cdot \Delta\mathbf{d} \tag{2}$$

Where $\mathbf{S} \in \mathbb{R}^{N_n \times N_n}$ is the sensitivity matrix which contains information interrelating the variation of pressures in all the nodes caused by a variation of the demand.

A sensor placement approach, based on the analysis of the sensitivity matrix [5] must be applied to find the locations where the pressure is more sensible to the demand. Equation (3) represents a sensor placement process to find the optimal sensor ubications given the sensitivity matrix $\mathbf{S}$ and the number of sensors $N_s$.

$$Sensor\ Placement(\mathbf{S}(B_{Cond}, \mathbf{d}), N_s) = \mathbf{Id}^* \tag{3}$$

Where $\mathbf{Id}^* \in \mathbb{N}^{N_s}$ is the index of the nodes of the optimal sensor locations.

The number of sensors distributed on the WDN in these layouts must be below a budget limit defined as $N_s \leq N_{sMax}$.

Once the possible sensors layouts with different number of sensors $N_s$ have been determined, the optimal number of sensors $N_s{}^*$ must be stablished. To determine the optimal number of sensors, an indicator must be defined and used to quantify the degree of relevance of the information recorded by a sensor layout. This indicator is defined as $\Delta\hat{\mathbf{p}}_{\boldsymbol{meas}} \in \mathbb{R}^{N_n}$ as presented in Equation (4). Its computation will be presented in the methodology section.

$$Information\ of\ Instrumentation\ Indicator(\mathbf{Id}^*) = \Delta\hat{\mathbf{p}}_{\boldsymbol{meas}} \tag{4}$$

To determine the optimal number of sensors $N_s{}^*$, the indicator $\Delta\hat{\mathbf{p}}_{\boldsymbol{meas}}$ will be computed and evaluated for all the feasible layouts of sensors such that $N_s \leq N_{sMax}$ until the increase of the number of sensors does not increase the indicator quantifying the relevance of the information recorded by them. Equation (5) represents the trade-off used to find optimal number of sensors $N_s{}^*$ from which the weighted increase of the indicator does not compensate the increase in the cost of the sampling design $C_{Sensor}$.

$$W(mean(\Delta\hat{\mathbf{p}}_{\boldsymbol{meas}}(N_s{}^* + 1)) - mean(\Delta\hat{\mathbf{p}}_{\boldsymbol{meas}}(N_s{}^*))) < C_{Sensor} \tag{5}$$

## 3 CASE STUDY

Terrassa's WDN is divided into eight pressure floors. The division is performed by minimizing the altitude variation within these pressure floors to ease the management and efficiency. As the altitude variations within these floors are reasonable, the floors can be supplied mainly by gravity from tanks. The company have generated eight hydraulic models of these pressure floors and intends to calibrate these models.

The results presented in [4](Water Distribution Network Model calibration and Continuous Maintenance: Terrassa, a real application) validated the physical model of the pressure floor of Sulleva to generate models of type one and type two. To generate a type three model a microcalibration process will be performed. This microcalibration process requires more instrumentation installed in the WDN.

The WDN of Sulleva consist of 32,2 km of pipes and supplies approximately 530.000 m3/year to 4.500 users. The pressure floor is gravity-fed from a single tank and is instrumented with five flow meters dividing the WDN in its four DMAs. The two lower DMAs are separated by a pressure reducing valve (PRV) from the two upstream DMA. Figure 1 presents the hydraulic model of the pressure floor of Sulleva. The water source is the reservoir signalled with a blue square. The boundaries of the four DMAs are defined by the flowmeters, signalled by green squares, and by closed valves, signalled by black squares. The PRV separating the two upper DMAs from the two lower DMAs is signalled with a red square. The pipes of the two upper DMAs are signalled in black and the pipes of the two lower DMAs are signalled in magenta.

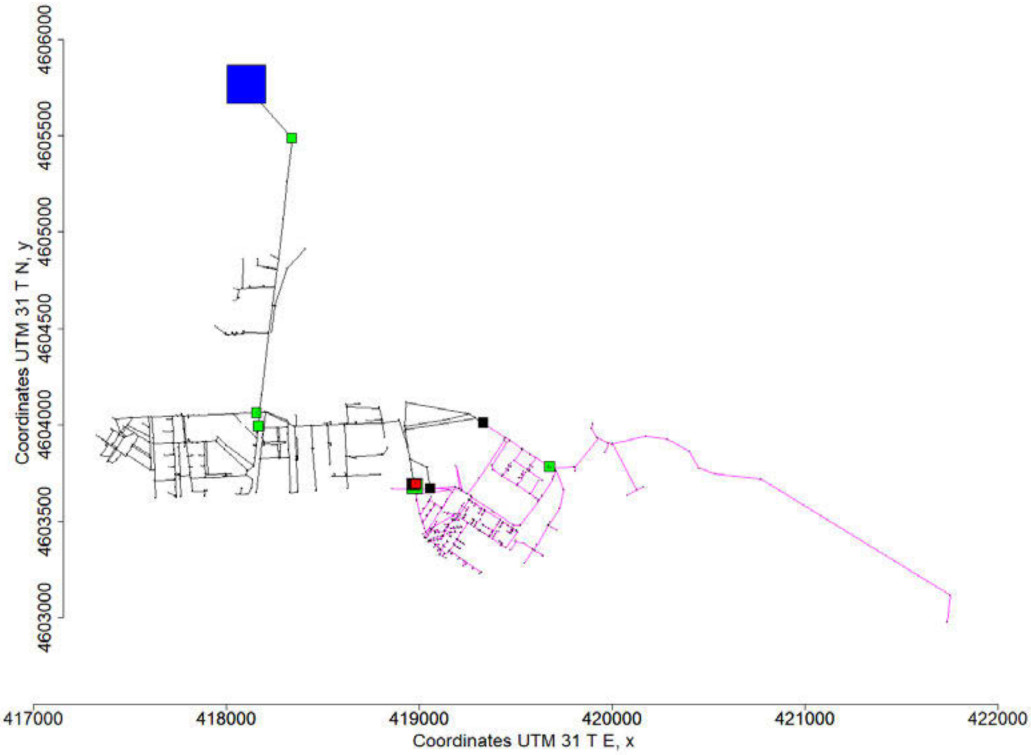


*Figure 1. WDN model of Sulleva pressure floor.*

As one of the flow meters and a pressure sensor are located at the outlet of the PRV, the WDN model is divided in two models to avoid including the PRV in the sensitivity matrices computation. In the upstream of the PRV model, the PRV is substituted by a consumption node and the demand of the node is fixed according to the flow measured by the flow meter located at the outlet of the PRV. In the downstream of the PRV model, the PRV is substituted by a reservoir whose hydraulic head is fixed according to the measurements of the pressure sensor located at the outlet of the PRV.

In this work the sampling design methodology is applied only to the upstream of the PRV model and the results obtained are displayed to illustrate the procedure for applying the methodology to a specific WDN model. This WDN model contains 18,7 km of pipes, 573 links, 543 nodes and 115 consumption nodes.

# 4 METHODOLOGY AND RESULTS

## 4.1 Simulation for the Sampling Design

Usually, to model the demands the users of the same type are assumed to have similar diurnal pattern and the consumption of each user is computed by multiplying the pattern coefficients with the baseline demand as presented in [19]. However, user diurnal patterns are not always available in practice. Quite often, water companies only manage information with low temporal resolution, the monthly or quarterly billing of each consumer. This information can be used to compute the baseline demand or base demand of each user. Additional information collected from flow-meters recording all the water entering and leaving the DMAs may be used to estimate each user consumption at every instant. The basic model presented in Equation (6) uses the nodal base demand, together with the total DMA consumption metered at the DMA inlets to calculate the demand of each node at each sample.

$$\boldsymbol{d}_i(t) = \frac{bd_i}{\sum_{j=1}^{N_n} bd_j} \cdot \boldsymbol{q}_{\boldsymbol{in},\boldsymbol{DMA\ k}}(t) \tag{6}$$

Where $bd_i$ is the base demand of node $i$; and $\boldsymbol{q}_{\boldsymbol{in},\boldsymbol{DMA\ k}}(t)$ is the total DMA water consumption metered at sample $t$.

As no prior information about the diurnal pattern of consumption of the users is available, the information of the flowmeters measuring the inflows and outflows of the DMAs is used to model the demands of the users by means of equation (6) and generate a simulation that will be analysed to compute the sensitivity matrix at each working point and carry on the sampling design based on the model simulation.

## 4.2 Sensor Placement

Due to the large number of unknown values or parameters, it is impossible to calibrate the model of a real system precisely [20]. Kang and Lansey [21], [22] have emphasized the importance to make the model parameters identifiable by reducing the number of calibrated parameters to make the system overdetermined or at least even determined, as not sufficient measurements are available. The same conclusion was drawn from the Battle of the Water Calibration Networks, organized in 2010, pointing out that calibration size problem reduction is an important factor to consider to avoid model overfitting and unnecessary simulations reducing the search space [23]. Too much aggregation leads to few parameters that are easy to calibrate, but it also entails worse model predictions with significant errors. Increasing the number of calibrated parameters improves the agreement between model predictions and measurements, but parameter uncertainty increases too. Thus, the trade-off between model error due to aggregation of parameters and parameter uncertainty should be taken into account [24].

As the demands are intended to be calibrated by means of pressure measurements, the Singular Value Decomposition (SVD) to generate the right-singular vectors **V** is applied to the sensitivity matrix of the nodal pressures versus the demands presented as **S** in equation (2). Equation (7) show the SVD of **S**, where $\boldsymbol{\Sigma} \in \mathbb{R}^{N_n \times N_n}$ is a diagonal matrix containing the singular values of matrix **S** and $\mathbf{U} \in \mathbb{R}^{N_n \times N_n}$ and $\mathbf{V} \in \mathbb{R}^{N_n \times N_n}$ are the left and right singular vectors of matrix **S**.

$$SVD(\mathbf{S}) = \mathbf{U} \cdot \boldsymbol{\Sigma} \cdot \mathbf{V}^{\mathrm{T}} \tag{7}$$

Using **V** the resolution matrix **R** can be defined as equation (8).

$$\mathbf{R} = \mathbf{V} \cdot \mathbf{V}^{\mathrm{T}} \tag{8}$$

Applying the delta vector generation process to the parameter resolution matrix $\mathbf{R}$ the demands can be grouped depending on their resolvability [25], [26], [5]. This demand grouping approach tends to generate geographical groups as topological information is included in the sensitivity matrix [5].

The sampling design is performed according to a budget limit that sets a bound $N_{sMax}$ on $N_s$. Thus, the sensor placement methodology is applied for all the possible number of sensors satisfying $N_s \leq N_{sMax}$.

In the particular case of application $N_{sMax} = 6$. To illustrate the sensor placement methodology, the results for $N_s = 4$ are shown. To obtain an even determined system of equations guaranteeing the system identifiability the number of parameters must be equal to the number of sensors. Therefore, for $N_s = 4$ the demands are parametrized in four geographical groups of demands. Figure 2 represents the membership of each node to each of the demand groups obtained from applying the demand grouping approach at a particular working point of the EPS. Thus, the demand groups displayed are obtained analysing the sensitivity matrix computed at that specific working point (see Equation (2)).

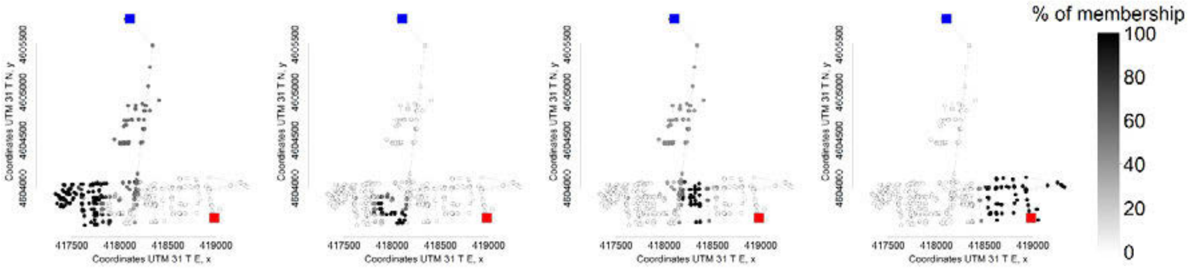


a) 1st Demand group b) 2nd Demand group c) 3rd Demand group d) 4th Demand group

*Figure 2. Nodal membership to demand groups.*

Maximizing the sensitivity is important in inverse problems because if the measurements are insensitive to the parameters, a large change in those parameters will change very little the measurements, perhaps within the error of measurement, and the parameters will be determined with low confidence [27].

As the groups of demands are intended to be calibrated by means of pressure measurements, a new sensitivity matrix of the nodal pressures versus the demand groups $\mathbf{S}' \in \mathbb{R}^{N_n \times N_s}$ is computed. Thus, SVD to generate the left-singular vectors $\mathbf{U}' \in \mathbb{R}^{N_n \times N_n}$ is applied to the sensitivity matrix $\mathbf{S}'$ (equation (9)).

$$SVD(\mathbf{S}') = \mathbf{U}' \cdot \mathbf{\Sigma}' \cdot \mathbf{V}'^{\mathrm{T}} \tag{9}$$

Using $\mathbf{U}'$ information density matrix $\mathbf{I}_d$ can be defined as

$$\mathbf{I}_d = \mathbf{U}' \cdot \mathbf{U}'^{\mathrm{T}} \tag{10}$$

Applying the delta vector generation process to the parameter information density matrix $\mathbf{I}_d$ the most sensible sensor locations to each demand group can be determined [25], [5].

To make the sensor placement more robust considering the temporal changes of the demands the sensor placement process is performed under unsteady hydraulic conditions by applying the process to each working point of an EPS (see equation (3)) [7], [16]. Thus, applying the sensor placement process to $k$ different working points, $k \cdot N_s$ possible locations of sensors are obtained, from which $N_s$ sensos must be selected, being $k$ the number of steps of the EPS analysed to perform the sensor placement. For the case presented in this paper $k = 96$. In most of the cases, the network topology has the highest impact on the sensitivity matrix and the sensors are placed at nearby locations when analysing different working points [7].

The procedure to select the $N_s$ final sensors consists of 4 steps:

1. Select the set of possible locations of sensors that, having an hydraulic separation between them of less than a predefined threshold according to the WDN dimensions, contain the maximum number of repetitions. Repetitions are the number of times that a location has been selected as one of the $k \cdot N_s$ possible locations of sensors.
2. For each possible location of sensor $s$ in the set, a weight $w_s$ is calculated depending on its number of repetitions and the distance $d$ to other possible locations of the set and repetitions $r_i$ of other possible $N_{Set}$ locations in the set (equation (11)).

$$w_s = \sum_{i=1}^{N_{Set}} \frac{r_i}{10^{\frac{d_{s,i}}{d_{Max}(s)}}} \tag{11}$$

   Where: $r_i$ is the number of repetitions of the possible locations of sensors $i$; $N_{Set}$ is the number of sensors in the set; $d_{s,i}$ is the distance between the possible locations of sensors $s$ and $i$; and $d_{Max}(s)$ is the maximum distance between the possible location of sensor $s$ and all other possible locations of sensors in the set.

3. The location of sensors in the set with highest weight is selected. All the other sensors are deleted from the possible locations of sensors and their number of repetitions is added to the selected sensor.
4. Repeat the process until $N_s$ locations of sensors are selected.

Figure 3 presents the process of selection of the $N_s = 4$ sensor locations among the $k \cdot N_s$ possible locations obtained applying the sensor placement process to $k$ different working points. The possible locations of sensors are signalled in green, the sets of possible locations of sensors are signalled in cyan and the selected locations of sensors are signalled in red.

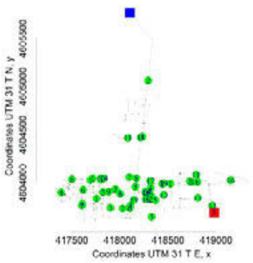

a) Possible locations of the sensors

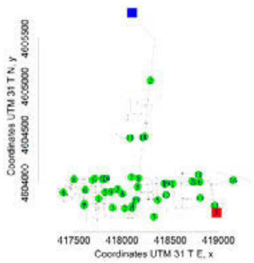

b) Possible locations of the sensors once 1st sensor is selected

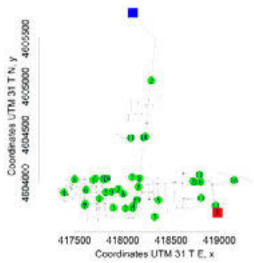

c) Possible locations of the sensors once 2nd sensor is selected

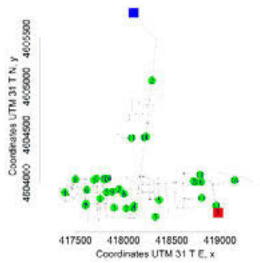

d) Possible locations of the sensors once 3rd sensor is selected

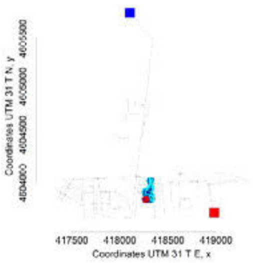

e) 1st sensors set and 1st sensor selected

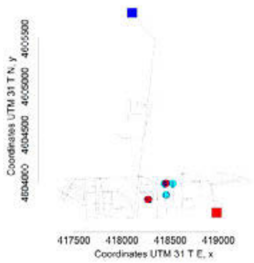

f) 2nd sensors set and 2nd sensor selected

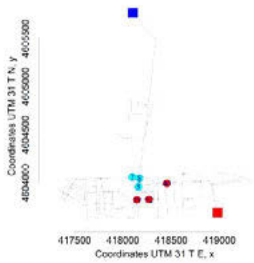

g) 3rd sensors set and 3rd sensor selected

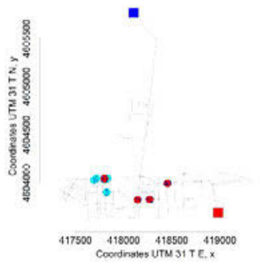

h) 4th sensors set and 4th sensor selected

*Figure 3. Process of selection of the locations of the sensors.*

## 4.3 Optimal Number of Sensors

It has been stated that to determine the optimal number of sensors it is necessary to define an indicator $\Delta\hat{\mathbf{p}}_{meas}$ that quantifies the relevance of the information recorded by a pressure sensor layout (see equation (4)). An easily interpretable indicator can be based on the effect that a demand variation have on pressure measurements. The indicator $\Delta\hat{\mathbf{p}}_{meas}$ is defined as the maximum variation of pressure that can be measured in the network given a fixed demand variation $\Delta d$ occurring at each node separately.

Once the indicator $\Delta\hat{\mathbf{p}}_{meas}$ is defined, it is necessary to define which must be the magnitude of these demand variation $\Delta d$ and which is an acceptable value for the pressure variations measured. To determine these magnitudes, an optimal scenario is defined in which the WDN is fully instrumented with pressure sensors located at all the nodes of the WDN model. In such scenario $\Delta d$ is defined as the minimum variation of demand that, occurring at any node of the WDN, would always be detectable. Detectable means that the produced pressure variation at any of the measurement locations is larger than the accuracy of the pressure sensors $\Delta p_{min}$

Pseudocode shown in Table 1 presents the procedure applied to determine $\Delta d$, where $\hat{\mathbf{p}}_{\mathbf{0}} \in \mathbb{R}^{N_n}$ is the nodal pressure vector at $\mathbf{d_0} \in \mathbb{R}^{N_n}$ reference working point; and $\Delta\hat{\mathbf{p}}_{meas}{}^{*} \in \mathbb{R}^{N_n}$ is the vector containing $N_n$ elements corresponding to the maximum variation of pressure measured when varying the demand of each node separately at the optimal scenario of a fully instrumentated WDN ($N_s = N_n$).

In line 3 of the pseudocode in Table 1, the first simulation at the $\mathbf{d_0}$ reference working point is performed and the nodal pressures obtained are stored in vector $\hat{\mathbf{p}}_{\mathbf{0}}$ (See Equation (1)). In lines 4 to 13 sets of $N_n$ simulations are performed by increasing the demand of each node separately by $\Delta d$. In line 9 the nodal pressures obtained from these simulations are stored in vector $\hat{\mathbf{p}}_{\mathbf{var}}$. In line 10 the maximum variations of pressure produced at each of the $N_n$ simulations varying the consumption of each node separately are stored in vector $\Delta\hat{\mathbf{p}}_{meas}{}^{*}$ at index of the node whose demand is varied. The while loop applied in line 4 sets a terminating condition which consist in breaking the loop if each of the maximum variation of pressure caused by each of the variation of demand is larger than the sensor accuracy $\Delta p_{min}$ for all the $N_n$ simulations. Therefore, considering the sensor accuracy, a variation of demand of magnitude $\Delta d$ applied at any node would be detected in the hypothetical scenario of having sensors installed at all the nodes of the WDN model. If it is not the case, the magnitude of the variation of the demand $\Delta d$ is increased and more set of $N_n$ simulations are performed until the terminating condition is fulfilled.

The functions $min()$ and $max()$ in tables 1 and 2 return the minimum and maximum element of a given vector respectively. The function $abs()$ in tables 1 and 2 returns a vector containing the absolute value of each element of a given vector and the operator $\boldsymbol{vector}(j)$ is accessing to the $j^{\text{th}}$ element of the given vector.

*Table 1. Pseudocode to determine the magnitude of the variation of the demand and the optimal information of instrumentation indicator [Caption, Cambria, 10pt, Italic, centred]*

| **Pseudocode to determine the magnitude of the variation of the demand and the optimal information of instrumentation indicator** | |
|---|---|
| **Require:** WDN model, $\mathbf{d_0}$, $\Delta p_{min}$ | **Return:** $\Delta d$, $\Delta\hat{\mathbf{p}}_{\boldsymbol{meas}}^{*}$ |
| $i = 0$ | |
| $\Delta\hat{\mathbf{p}}_{\boldsymbol{meas}}^{*} = \mathbf{0}$ | |
| $\hat{\mathbf{p}}_{\mathbf{0}} = Simulate\ Model(\mathbf{d_0})$ | |
| **While** $min(\Delta\hat{\mathbf{p}}_{\boldsymbol{meas}}^{*}) \leq \Delta p_{min}$: | |
|     $i = i + 1$ | |
|     $\Delta d = i \cdot \delta$ | |
|     **For** $j = 1 : N_n$ **do** | |
|         $\mathbf{d_{var}} = \mathbf{d_0}$ | |
|         $\mathbf{d_{var}}(j) = \mathbf{d_0}(j) + \Delta d$ | |
|         $\hat{\mathbf{p}}_{\mathbf{var}} = Simulate\ Model(\mathbf{d_{var}})$ | |
|         $\Delta\hat{\mathbf{p}}_{\boldsymbol{meas}}^{*}(j) = max(abs(\hat{\mathbf{p}}_{\mathbf{0}} - \hat{\mathbf{p}}_{\mathbf{var}}))$ | |
|     **End for** | |
| **End while** | |
| **Return:** $\Delta d$, $\Delta\hat{\mathbf{p}}_{\boldsymbol{meas}}^{*}$ | |

The pressure sensors that are installed by applying the sampling design approach presented in this paper have an accuracy of ± 1 cmH2O. Thus, the sensor accuracy $\Delta p_{min}$ is set to 1 cmH2O. The procedure presented in pseudocode of table 1 to the studied WDN gives a magnitude of the variation of the nodal demand of $\Delta d = 0{,}17$ L/s. Figure 4 illustrates how increasing the magnitude of $\Delta d$, the number of nodes whose demand variation is detectable increases for the studied WDN. The nodes signalled by green represent the nodes whose demand variation causes a detectable pressure variation. The nodes signalled by red represent the nodes whose demand variation causes too small pressure variations for being detectable.

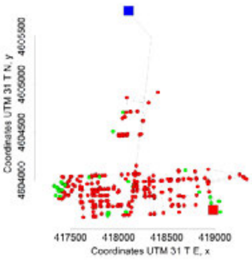


a) $\Delta d = 0.05$ L/s

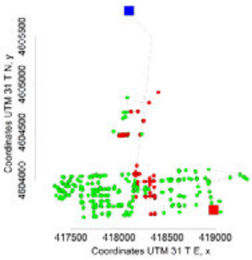


b) $\Delta d = 0.1$ L/s

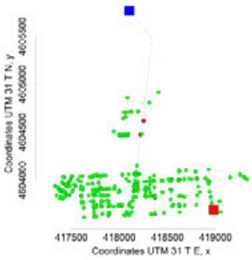


c) $\Delta d = 0.15$ L/s

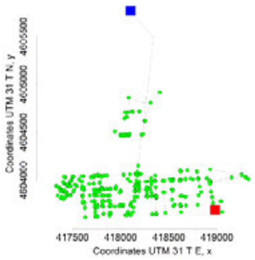


d) $\Delta d = 0.17$ L/s

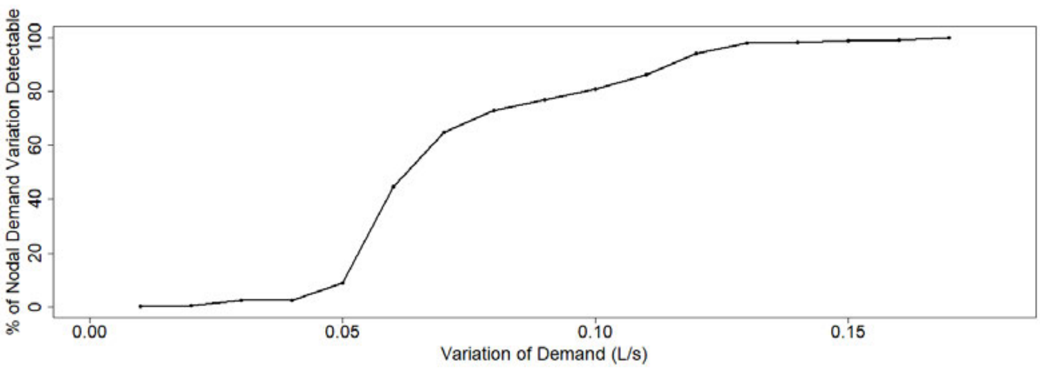


e) Percentage of nodal demand variation detectable depending on the magnitude of $\Delta d$

*Figure 4. Nodal demand variation detectable depending on the magnitude of Δd.*

The second output of the pseudocode of table 1 is the nodal vector $\mathbf{\Delta\hat{p}}_{meas}{}^{*}$ corresponding to the maximum pressure variation caused by each nodal demand variation separately. Figure 5 is the plot of the $\mathbf{\Delta\hat{p}}_{meas}{}^{*}$. It associates each component of $\mathbf{\Delta\hat{p}}_{meas}{}^{*}$ to the node whose nodal demand variation is causing that pressure variation. This figure displays the indicator that quantifies the relevance of the information recorded at optimal situation in which the WDN is fully instrumented with pressure sensors at each node ($N_s = N_n$). The indicator computed for the optimal scenario is useful to appreciate which areas of the network have room for improvement when comparing with the indicator computed for feasible layouts of sensors.

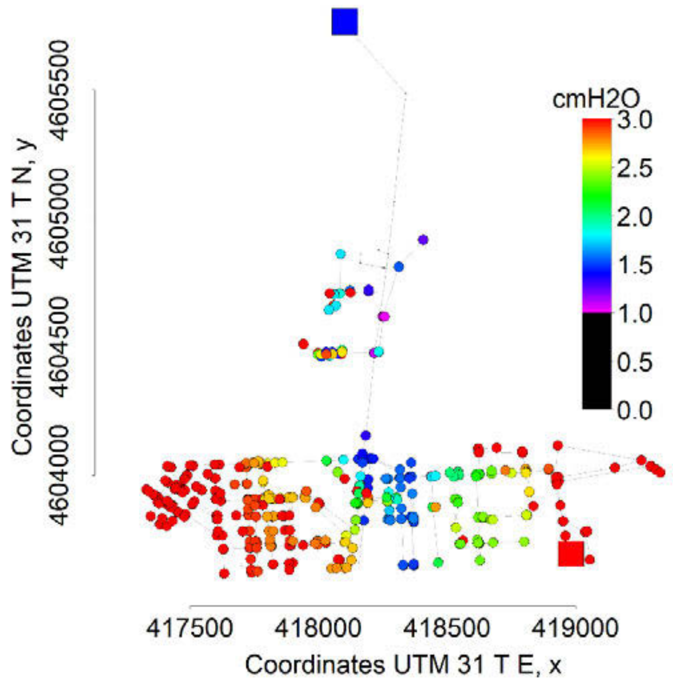


*Figure 5. Maximum pressure variation measurable $\hat{\boldsymbol{\Delta}}\boldsymbol{p}_{meas}{}^{*}$ for a fully instrumented WDN ($N_s = N_n$).*

To generate the indicator $\hat{\boldsymbol{\Delta}}\mathbf{p}_{meas}$, only the pressure variations produced at the locations of the sensors must be considered.

The process to generate the indicator $\hat{\boldsymbol{\Delta}}\mathbf{p}_{meas}$ consists in performing $N_n + 1$ simulations,. The first simulation corresponds to the working point $\mathbf{d_0}$ with respect to which the variation of pressures measured by the sensors will be analysed. The following $N_n$ simulations represent a variation of demand applied on each node separately. Thus, comparing the pressures obtained from the $N_n$ simulations with respect to the pressures obtained from the first simulation considering that only the pressures at the locations of the sensors will be known, the maximum variations of pressures that could be measured can be obtained.

Pseudocode presented in Table 2 corresponds to the process generating the indicator $\hat{\boldsymbol{\Delta}}\mathbf{p}_{meas}$ as the maximum pressure variations are searched only among the locations of the sensors. Notice that the execution of the first and the last $N_n$ simulations of the pseudocode presented in table 1 are equivalent to the $N_n + 1$ simulations executed in pseudocode presented in table 2 if the magnitude of the variation of the nodal demand $\Delta d$ is fixed according to the output of pseudocode presented in table 1.

*Table 2. Pseudocode to determine the maximum pressure variation detectable for a given layout of sensors caused by each nodal demand variation separately*

| $Information\ of\ Instrumentation\ Indicator$ | |
|---|---|
| **Require:** WDN model, $\mathbf{d_0}$, $\Delta d$, $\mathbf{Id}^*$ | **Return:** $\boldsymbol{\Delta\hat{p}_{meas}}$ |

$\boldsymbol{\Delta\hat{p}_{meas}} = \mathbf{0}$;
$\mathbf{\hat{p}_0} = Simulate\ Model(\mathbf{d_0})$**;**
**For** $j = 1: N_n$ **do**
    $\mathbf{d_{var}} = \mathbf{d_0}$
    $\mathbf{d_{var}}(j) = \mathbf{d_0}(j) + \Delta d$
    $\mathbf{\hat{p}_{var}} = Simulate\ Model(\mathbf{d_{var}})$**;**
    $\boldsymbol{\Delta\hat{p}_{meas}}(j) = max(abs(\mathbf{\hat{p}_0}(\mathbf{Id}^*) - \mathbf{\hat{p}_{var}}(\mathbf{Id}^*)))$;
**End for**
**Return:** $\boldsymbol{\Delta\hat{p}_{meas}}$

It is expected that for a reduced number of sensors distributed on the WDN increasing the number of sensors will significantly increase the magnitude of the maximum variation of pressures measured by the sensors. However, it is also expected to reach a certain number of sensors from which increasing the number of sensors distributed on the WDN does not significantly increase the magnitude of the maximum variation of pressures measured by the sensors.

Finally, to determine the optimal layout of pressure sensors both processes, the sensor placement and optimal number of sensors definition, must be applied. Initially, the first methodology locating the sensors is applied for different number of sensors to obtain several possible layouts of sensors. Thus, the second methodology quantifying the optimality of a layout of sensors is applied to decide which of the previously obtained layout is the most appropriate for the specific WDN being studied. These sampling design methodologies can adapt according to a budget, as the maximum number of sensors distributed on the network can be limited.

Figure 6 presents the results of applying the entire sampling design methodology. The sensor placement is applied for several predefined $N_s$ number of sensors from one to six according to the budget limit. The locations of the sensors are signalled by orange squares. Thus, the optimal number of sensor process is applied to generate the indicator $\boldsymbol{\Delta\hat{p}_{meas}}$ given the six different layouts of sensors obtained from the sensor placement process.

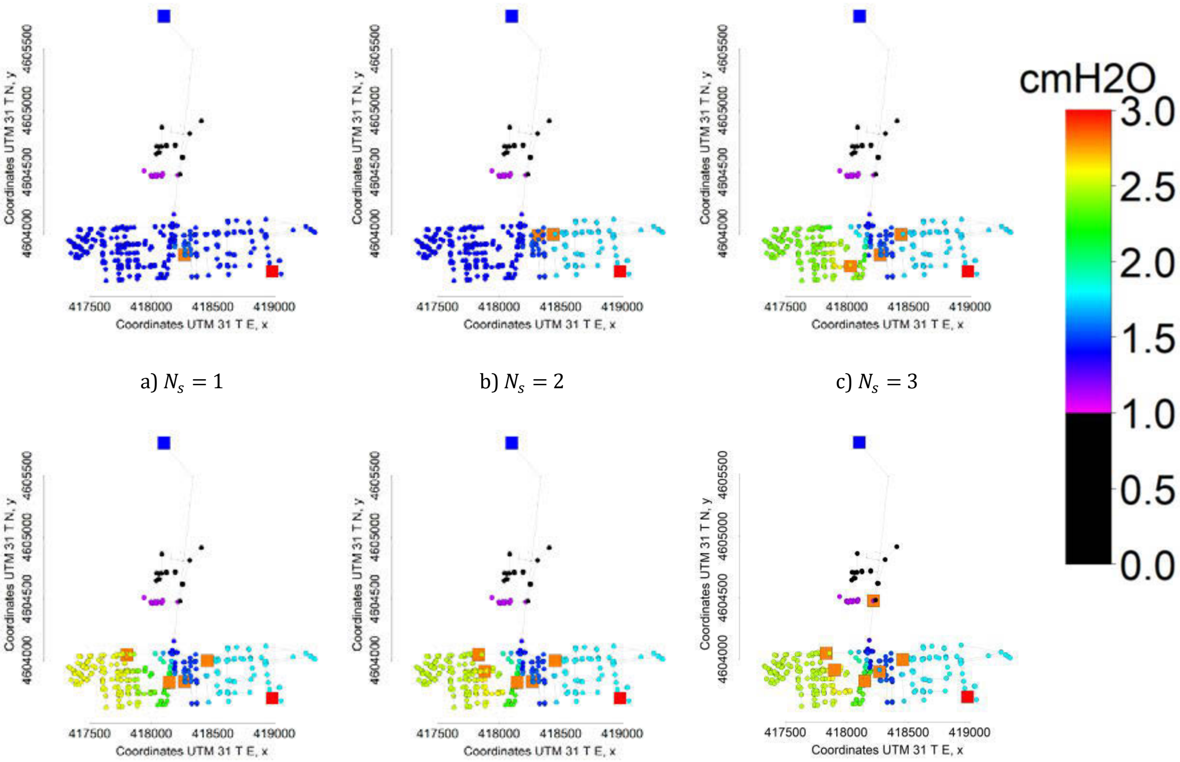


a) $N_s = 1$ b) $N_s = 2$ c) $N_s = 3$

a) $N_s = 4$ b) $N_s = 5$ c) $N_s = 6$

*Figure 6. Maximum pressure variation measurable $\boldsymbol{\Delta p_{meas}}$ for feasible number of sensors $N_s \leq N_{sMax}$.*

Figure 7 displays the mean of all the maximum variation of pressures measurable by the sensors given the six different layouts of sensors. It can be appreciated that distributing five or six pressure sensors with the sensor placement procedure applied does not significantly increase the magnitude of the maximum variation of pressures that would be measured by the sensors with respect to the layout using four sensors. For this reason, the optimal number of sensors to be installed is set to four.

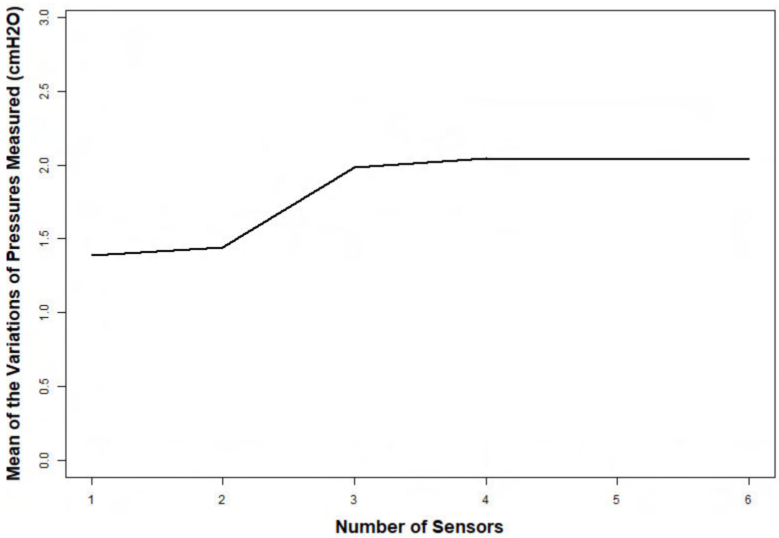


*Figure 7. Mean of maximum pressure variation measured $\boldsymbol{\Delta p_{meas}}$ for feasible number of sensors $N_s \leq N_{sMax}$.*

## 5 CONCLUSIONS

This work has presented a complete model-based methodology to determine an optimal pressure sensor placement layout and the appropriate number of pressure sensors to install on a WDN.The methodology uses a sensor placement methodology from the literature that finds the most sensible locations with respect to demand groups. Additionally, to determine the optimal number of sensors a new methodology that can be interpretable by the company has been developed with the aim to overcome the gap between research and practice. The sampling design methodology is able to adapt to a budget as the maximum number of sensors distributed on the network can be limited.

This methodology has been developed within an instrumentation project plan of TAIGUA. That has been successfully applied to several real WDN and the company is installing pressure sensors according to the layouts of sensors obtained. Results illustrating this application have been displayed.

With the information recorded by the new sensors it is intended to microcalibrate the demand of the WDN models and implement a leak-detection and localization approach that can be coupled with the demand calibration methodology. Additionally, the calibrated WDN model and a precise demand model can be used to enhance the energetic and economic efficiency of the operational control of the WDN.

## 6 REFERENCES


[1] R. Wéber and C. Hős, "Efficient Technique for Pipe Roughness Calibration and Sensor Placement for Water Distribution Systems," J. Water Resour. Plan. Manag., vol. 146, no. 1, p. 04019070, Jan. 2020, doi: 10.1061/(ASCE)WR.1943-5452.0001150.

[2] Perez, Ramon; Sanz, Gerard; Cuguero, Josep; and Cuguero, Miquel Angel, "Optimal Placement Of Metering Devices For Multiple Purposes", CUNY Academic Works, 2014.

[3] L. E. Ormsbee and S. Lingireddy, "Calibrating hydraulic network models," J. Am. Water Works Assoc., vol. 89, no. 2, pp. 42–50, Feb. 1997, doi: 10.1002/j.1551-8833.1997.tb08177.x.

[4] Ramon Pérez R., Cugueró J., Romera J., Van Eeckhout J., Cabot J., Franch O., "Water Distribution Network Model Calibration and Continuous Maintenance : Terrassa , A Real Application," Modern Environmental Science and Engineering., vol. 7, no. 9, pp. 891-897, 2021, doi: 10.15341/mese(2333-2581)/09.07.2021/003.

[5] G. Sanz and R. Pérez, "Sensitivity Analysis for Sampling Design and Demand Calibration in Water Distribution Networks Using the Singular Value Decomposition," J. Water Resour. Plan. Manag., vol. 141, no. 10, p. 04015020, Oct. 2015, doi: 10.1061/(ASCE)WR.1943-5452.0000535.

[6] T. Walski, P. Sage, and Z. Wu, "What Does it Take to Make Automated Calibration Find Closed Valves and Leaks?," in World Environmental and Water Resources Congress 2014: Water Without Borders - Proceedings of the 2014 World Environmental and Water Resources Congress, 2014, pp. 555–565, doi: 10.1061/9780784413548.059.

[7] G. Sanz and R. Pérez, "Comparison of demand calibration in water distribution networks using pressure and flow sensors," Procedia Eng., vol. 119, no. 1, pp. 771–780, 2015, doi: 10.1016/j.proeng.2015.08.933.

[8] "ADT1 remote transmission units with data loggers from Keller manufacturer." https://keller-druck.com/en/products/wireless-solutions/remote-transmission-units/adt1-box.

[9] G. Yu and R. S. Powell, "Optimal design of meter placement in water distribution systems," Int. J. Syst. Sci., vol. 25, no. 12, pp. 2155–2166, 1994, doi: 10.1080/00207729408949342.

[10] R. W. Meier and B. D. Barkdoll, "Sampling Design for Network Model Calibration Using Genetic Algorithms," J. Water Resour. Plan. Manag., vol. 126, no. 4, pp. 245–250, Jul. 2000, doi: 10.1061/(ASCE)0733-9496(2000)126:4(245).

[11] W. B. F. De Schaetzen, G. A. Walters, and D. A. Savic, "Optimal sampling design for model calibration using shortest path, genetic and entropy algorithms," Urban Water, vol. 2, no. 2, pp. 141–152, 2000, doi: 10.1016/s1462-0758(00)00052-2.

[12] Z. S. Kapelan, D. A. Savic, and G. A. Walters, "Multiobjective Sampling Design for Water Distribution Model Calibration," J. Water Resour. Plan. Manag., vol. 129, no. 6, pp. 466–479, Nov. 2003, doi: 10.1061/(ASCE)0733-9496(2003)129:6(466).

[13] J. P. Vtkovský, J. A. Liggett, A. R. Simpson, and M. F. Lambert, "Optimal Measurement Site Locations for Inverse Transient Analysis in Pipe Networks," J. Water Resour. Plan. Manag., vol. 129, no. 6, pp. 480–492, Nov. 2003, doi: 10.1061/(ASCE)0733-9496(2003)129:6(480).

[14] Z. S. Kapelan, D. A. Savic, and G. A. Walters, "Optimal Sampling Design Methodologies for Water Distribution Model Calibration," J. Hydraul. Eng., vol. 131, no. 3, 2005, doi: 10.1061/(asce)0733-9429(2005)131:3(190).

[15] K. Behzadian, Z. Kapelan, D. Savic, and A. Ardeshir, "Stochastic sampling design using a multi-objective genetic algorithm and adaptive neural networks," Environ. Model. Softw., vol. 24, no. 4, pp. 530–541, Apr. 2009, doi: 10.1016/j.envsoft.2008.09.013.

[16] D. Kang and K. Lansey, "Optimal Meter Placement for Water Distribution System State Estimation," J. Water Resour. Plan. Manag., vol. 136, no. 3, pp. 337–347, 2010, doi: 10.1061/(asce)wr.1943-5452.0000037.

[17] D. A. Savic, Z. S. Kapelan, and P. M. R. Jonkergouw, "Quo vadis water distribution model calibration?," Urban Water J., vol. 6, no. 1, pp. 3–22, 2009, doi: 10.1080/15730620802613380.

[18] G. Sanz, R. Pérez, Z. Kapelan, and D. Savic, "Leak Detection and Localization through Demand Components Calibration," J. Water Resour. Plan. Manag., vol. 142, no. 2, p. 04015057, 2016, doi: 10.1061/(asce)wr.1943-5452.0000592.

[19] G. Sanz and R. Pérez, "Demand Pattern Calibration in Water Distribution Networks," Procedia Eng., vol. 70, pp. 1495–1504, 2014, doi: 10.1016/j.proeng.2014.02.164.

[20] T. M. Walski, "Model calibration data: The good, the bad, and the useless," J. / Am. Water Work. Assoc., vol. 92, no. 1, pp. 94–99, 2000, doi: 10.1002/j.1551-8833.2000.tb08791.x.

[21] D. Kang and K. Lansey, "Real-Time Demand Estimation and Confidence Limit Analysis for Water Distribution Systems," J. Hydraul. Eng., vol. 135, no. 10, pp. 825–837, Oct. 2009, doi: 10.1061/(ASCE)HY.1943-7900.0000086.

[22] D. Kang and K. Lansey, "Demand and Roughness Estimation in Water Distribution Systems," J. Water Resour. Plan. Manag., vol. 137, no. 1, pp. 20–30, Jan. 2011, doi: 10.1061/(ASCE)WR.1943-5452.0000086.

[23] A. Ostfeld et al., "Battle of the Water Calibration Networks," J. Water Resour. Plan. Manag., vol. 138, no. 5, pp. 523–532, Sep. 2012, doi: 10.1061/(ASCE)WR.1943-5452.0000191.

[24] K. N. Mallick, I. Ahmed, K. S. Tickle, and K. E. Lansey, "Determining Pipe Groupings for Water Distribution Networks," J. Water Resour. Plan. Manag., vol. 128, no. 2, pp. 130–139, Mar. 2002, doi: 10.1061/(ASCE)0733-9496(2002)128:2(130).

[25] R. A. Wiggins, "The general linear inverse problem: Implication of surface waves and free oscillations for Earth structure," Rev. Geophys., vol. 10, no. 1, pp. 251–285, 1972, doi: 10.1029/RG010i001p00251.

[26] R. C. Aster, B. Borchers, and C. H. Thurber, Parameter Estimation and Inverse Problems. Elsevier, 2019.

[27] J. A. Liggett and L. Chen, "Inverse Transient Analysis in Pipe Networks," J. Hydraul. Eng., vol. 120, no. 8, pp. 934–955, Aug. 1994, doi: 10.1061/(ASCE)0733-9429(1994)120:8(934).